

# Laser operation of an Nd:Gd<sub>3</sub>Ga<sub>5</sub>O<sub>12</sub> thin-film optical waveguide fabricated by pulsed laser deposition

Devinder S. Gill,<sup>a)</sup> Andrew A. Anderson, Robert W. Eason,<sup>b)</sup> T. J. Warburton, and D. P. Shepherd

*Optoelectronics Research Centre and Department of Physics, Southampton University, Southampton SO17 1BJ, United Kingdom*

(Received 26 February 1996; accepted for publication 29 April 1996)

We report the laser operation of a thin-film waveguide structure grown by the pulsed laser deposition technique. A 2.7- $\mu\text{m}$ -thick crystalline film of neodymium doped Gd<sub>3</sub>Ga<sub>5</sub>O<sub>12</sub> (Nd:GGG) lases at a wavelength centered at 1.06  $\mu\text{m}$  when pumped by a Ti:sapphire laser at 808 nm. © 1996 American Institute of Physics. [S0003-6951(96)03827-2]

Waveguide lasers are desirable because of the large intensity-length product and good pump and signal mode overlap, which can be achieved in the waveguide geometry. It can lead to a reduced pump power threshold compared to bulk lasers. Diode lasers are very suitable for pumping and for compact solid-state devices, provided the waveguide losses are low. Since propagation losses in a waveguide are generally quite high, (the lowest reported loss in a film fabricated by pulsed laser deposition (PLD) is  $\approx 1$  dB/cm,<sup>1</sup> waveguide lasers are most suitable for three-level or quasi-three-level laser systems which have high power thresholds due to reabsorption of the laser light by population within the lower laser level.<sup>2</sup> In this case, the propagation loss in the waveguide is not significantly greater than that present throughout the equivalent length of bulk crystal due to this additional absorption loss.

To date, ion implantation has been the principle technique for fabricating planar and channel waveguides within laser-gain media such as Nd:Y<sub>3</sub>Al<sub>5</sub>O<sub>12</sub> (Nd:YAG),<sup>3,4</sup> and Nd:Gd<sub>3</sub>Ga<sub>5</sub>O<sub>12</sub>,<sup>5,6</sup> with reported propagation losses  $\approx 1$  dB/cm. In addition, epitaxial growth methods such as liquid phase epitaxy,<sup>7</sup> and metalorganic chemical vapor deposition<sup>8</sup> have been employed for growing Nd:YAG layers on YAG and GGG substrates, respectively. The problems with these techniques, however, are the high costs associated with ion implantation and the lack of versatility offered by both liquid phase epitaxy and metalorganic chemical vapor deposition.

Recently, we have grown crystalline layers of undoped GGG on heated YAG substrates by the PLD technique. Waveguiding was demonstrated using a prism coupler and the effective refractive indices of the modes were evaluated.<sup>9</sup> PLD has emerged as a fast and versatile alternative to established thin-film growth techniques while still having the capability of growing high-quality single-crystal layers of the correct composition. There has only been one other report on the growth of crystalline laser-host garnets by PLD;<sup>10</sup> this was the deposition of Nd:YAG onto heated Si, MgO, and GGG substrates. In this case no waveguiding was possible due to the inappropriate choice of refractive indices.

In this letter we report on the fabrication of a neodymium doped GGG thin film on a single-crystal (444) YAG

substrate using the PLD technique, the spectroscopic and the lasing properties of this layer. To our knowledge, there have been no other reports of the successful operation of a waveguide laser fabricated by this technique.

The films were grown by ablating a 1 at. % Nd doped GGG ceramic target. (obtained from Testbourne Ltd., U.K.), with a KrF excimer laser operating at a wavelength  $\lambda=248$  nm. The fabrication process and deposition conditions have been described in detail in an earlier publication.<sup>9</sup> The one improvement to the process was the rigorous cleaning procedure which all the YAG substrates were put through in order to minimize the defects in the epitaxial layer. The substrates were rinsed in lotoxane, acetone, and isopropanol in an ultrasonic bath to remove any organic residue. They were then immersed in a mixture of H<sub>2</sub>SO<sub>4</sub> and H<sub>2</sub>O<sub>2</sub> for 20 min at 80 °C, followed by baking overnight at 120 °C to remove the excess water. Single-crystal YAG was chosen as a suitable substrate because it has a cubic structure with a room-temperature lattice spacing of 12.016 Å,<sup>11</sup> which corresponds to a lattice mismatch of only 2.9% between the film and substrate, (GGG is also cubic with a lattice spacing of 12.377 Å).<sup>11</sup> Also, both materials have similar thermal expansion coefficients, ( $\alpha_{\text{YAG}}=6.9\times 10^{-6}/\text{K}$  and  $\alpha_{\text{GGG}}=7.3\times 10^{-6}/\text{K}$ ,<sup>8</sup> thus minimizing the thermal tension at the interlayer boundary as the sample cools. Finally, YAG has a suitably lower refractive index than Nd:GGG, ( $n_{\text{YAG}}=1.816$  and  $n_{\text{GGG}}=1.965$  at  $\lambda=633$  nm),<sup>12</sup> so that propagating light can be confined in a narrow mode in the waveguide layer.

Figure 1 shows an x-ray diffraction spectrum of an Nd:GGG film deposited on a single-crystal (444) oriented YAG substrate. The film peak is located at an interplanar distance  $d=1.809$  Å which can be assigned to the (444) GGG peak, [the bulk crystal (444) peak has a lattice  $d$  spacing of 1.787 Å.<sup>13</sup>] The small discrepancy between the  $d$  spacings of the Nd:GGG layer and bulk crystal GGG is most probably due to the larger ionic radius of the Nd<sup>3+</sup> ion which can replace the Gd<sup>3+</sup> ion within the lattice, (0.995 Å compared with 0.938 Å for Gd<sup>3+</sup>).<sup>14</sup> Furthermore, the lattice mismatch between the film and substrate would induce a distortion of the Nd:GGG lattice structure at the interlayer boundary and may also be responsible for this slight discrepancy between the lattice  $d$  spacings. Notice from Fig. 1 that the GGG film peak is almost as narrow as the (444) YAG substrate peak which suggests that the film has a highly ordered structure. No additional peaks appeared on an ex-

<sup>a)</sup>Current address: Foundation for Research and Technology-Hellas (FO.R.T.H.), Institute of Electronic Structure and Laser (IESL), P.O. Box 1527, Heraklion 71110, Crete, Greece.

<sup>b)</sup>Corresponding author.

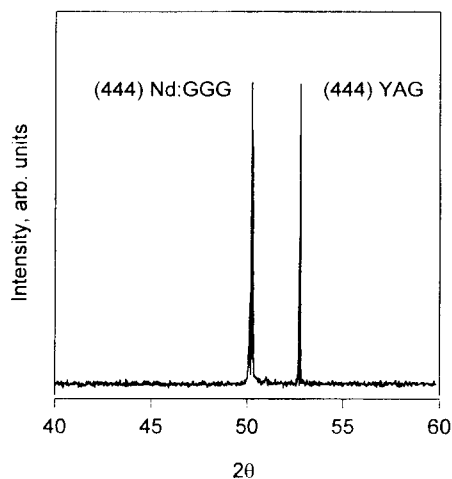


FIG. 1. X-ray diffraction spectrum of an Nd:GGG film deposited on a (444) YAG single-crystal substrate.

tended x-ray diffraction spectrum, (ranging from  $2\theta=2^\circ$  to  $75^\circ$ ), implying that the film has grown exclusively in the highly oriented (444) plane parallel to the (444) YAG surface.

The film shown in Fig. 1 had been grown for 30 min with the excimer laser operating at 20 Hz. It had a thickness of  $2.7 \mu\text{m}$ , measured with a Tencor alpha-step 2000 surface profiler. The guide should support three modes at the signal wavelength and four modes at the pump wavelength, ( $\lambda_p \approx 800 \text{ nm}$ ). Despite the higher threshold power associated with multimode waveguides, a relatively thick film, (i.e.,  $>2 \mu\text{m}$ ), is desirable because it greatly improves the coupling efficiency into the guide.

The propagation loss and coupling efficiency into the Nd:GGG layer was determined using the cutback method.<sup>15</sup> The transmission through an 8 and 1.25 mm guide was measured when launching light from a He-Ne, ( $\lambda=633 \text{ nm}$ ) into an end face using a  $\times 40$  objective. The end faces of the guide had been polished to an optically smooth finish to reduce the scattering losses. A transmission of 27% and 65% for the 8 and 1.25 mm samples, respectively, was calculated by taking into account Fresnel reflection losses ( $R_{in}=R_{out}=0.1$ ) and transmission losses through the objective lenses. It was thus calculated that the propagation loss in the waveguide was 6 dB/cm and the input coupling efficiency was 76%.

The spectroscopic properties of the neodymium ion were investigated by launching light from a Ti:sapphire laser into the Nd:GGG film using a  $\times 40$  objective lens. A chopper was positioned before the input lens and rotated at a speed such that the rise and fall times of the chopped pump radiation were less than the fluorescence lifetime of the  $\text{Nd}^{3+}$  ion. The output from the waveguide was detected with a photodiode and displayed on an oscilloscope. The fluorescence lifetime was determined directly from the signal on the oscilloscope and has a value in close agreement with the bulk crystal value of  $180 \mu\text{s}$ .<sup>5</sup>

The fluorescence spectrum of the Nd:GGG waveguide was recorded with an OMA2000 triple grating spectrometer (model 1235) and is displayed in Fig. 2. For comparison we have included the fluorescence spectrum obtained from a

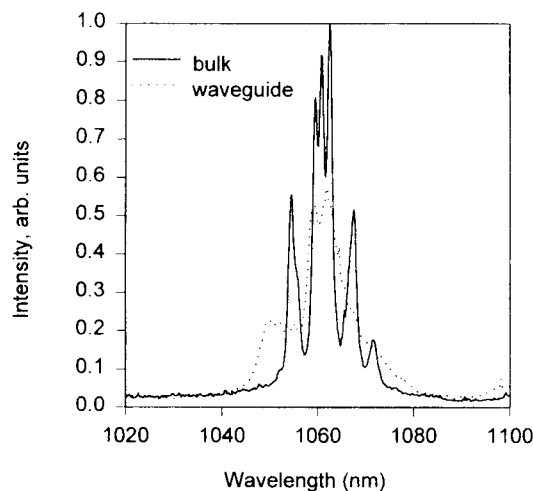


FIG. 2. Nd:GGG waveguide and bulk crystal fluorescence spectra in the  $1.06 \mu\text{m}$  region.

bulk crystal of Nd:GGG. It can be seen that there is a broadening of the waveguide peaks near the  $1.06 \mu\text{m}$  region which leads to a reduction in the peak emission cross section by a factor of 0.58. This factor of 0.58 can be estimated by comparing the peak heights in the bulk and the waveguide after plotting the spectra normalized to the same total area under all the fluorescence lines. Distortion in the local crystal field by intrinsic defects may be experienced by the neodymium ions resulting in this spectral broadening.

To investigate the lasing properties of the Nd:GGG film, it was necessary to cut the sample so that the propagating distance was only 1.25 mm. This is because the propagation losses were high (5.7 dB/cm), so that in longer samples the losses may have exceeded the gain in the cavity and precluded the onset of lasing. In addition, this comparatively short propagation length was well matched to the absorption depth of the pump wavelength. Despite this short length, the guided mode size of  $\approx 1 \mu\text{m}$  is still significantly smaller than the spot size for free space confocal focusing, ( $\approx 10 \mu\text{m}$ ). This is an important advantage gained from using a waveguide.

The end faces of the guide were polished to an optically smooth finish because even sub-micron sized chips and scratches would disturb the guided mode as it enters and exits the film, thus increasing the cavity loss. It was also necessary to produce highly parallel end faces to prevent "walk off" of the laser mode from the pumped region in the waveguide cavity with successive reflections. The parallelism was tested using both a He-Ne beam and a Logitech LG1 autocollimator.

Once again, radiation from the Ti:sapphire was launched into the guide using a  $\times 40$  objective lens. The laser cavity was created using two plane dielectric mirrors with high-reflectivity coatings (reflectivity  $>99.5\%$  at the signal wavelength of  $1.06 \mu\text{m}$ ), which were carefully butted onto the end faces of the guide and held by surface tension of a drop of Fluorinert FC-70 fluorinated liquid. The output was detected using a photodiode and displayed on an oscilloscope. At a threshold power of 190 mW incident on the input objective lens the onset of lasing was recorded, which corresponds to

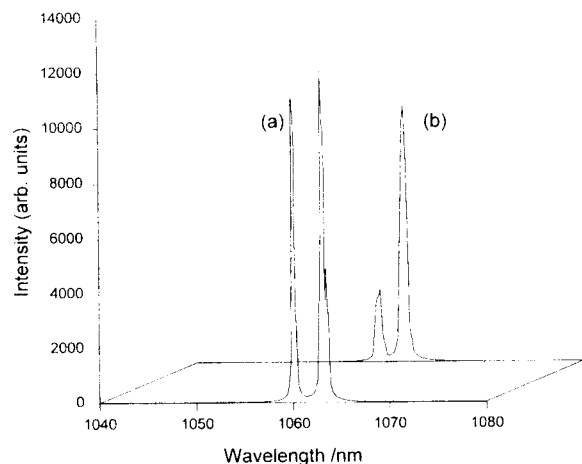


FIG. 3. The lasing spectra of the Nd:GGG waveguide laser. It can lase simultaneously at (a) 1.059 and 1.062  $\mu\text{m}$  or at (b) 1.06 and 1.063  $\mu\text{m}$ .

91 mW absorbed power, by taking into account the objective and mirror transmissions (71% and 89%, respectively), and a launch efficiency of 76%. The optimum pump wavelength was found to be 808.1 nm which lies in the strongest absorption band of the bulk crystal.<sup>5</sup> The absorption of the pump beam through the guide was calculated to be  $660 \text{ m}^{-1}$ . The maximum laser output from this waveguide structure, using two high-reflectivity mirrors was recorded as 800  $\mu\text{W}$ . The replacement of one of the high-reflectivity mirrors with a 2% output coupler increased the absorbed power threshold to nearly 192 mW. However, there was no sufficiently powerful pump source available to make a slope efficiency measurement.

Two typical lasing spectra of the Nd:GGG waveguide are shown in Fig. 3. It can be seen that the waveguide can lase at several different wavelengths due to the broadened fluorescence spectrum near 1.06  $\mu\text{m}$ . For example, the waveguide can lase simultaneously at 1.059  $\mu\text{m}$  and 1.062  $\mu\text{m}$  [as shown in Fig. 3(a)]. By altering the position of the pump beam it can also lase simultaneously at 1.06 and 1.063  $\mu\text{m}$  [as shown in Fig. 3(b)]. We found that these peaks were not polarization dependent. An ion-implanted Nd:YAG planar waveguide has been reported to lase simultaneously at 1.062 and 1.064  $\mu\text{m}$  and this effect was also attributed to a broadened fluorescence peak due to the implantation process.<sup>3</sup>

The waveguide laser output was imaged on a beam view analyzer (Big Sky Software Corporation). The beam had approximate Gaussian profiles in both planes of the guide and the divergence in each plane was recorded. The spot size in the guided plane was calculated as 1.5  $\mu\text{m}$  and the spot size in the unguided plane was averaged along the crystal length corresponding to a value of 16.8  $\mu\text{m}$ . Similarly, the spot size of the pump beam was calculated as 1.3  $\mu\text{m}$  in the vertical plane and the averaged spot size in the horizontal plane was calculated as 45  $\mu\text{m}$ .

A rough estimate of the absorbed threshold power can be obtained from the calculated pump and signal spot sizes using the equation below,<sup>16</sup>

$$P_{\text{th}} = \left( \frac{\pi h \nu_p}{2 \sigma_e \eta_p \tau_{\text{fl}}} \right) (W_{\text{lx}}^2 + W_{\text{px}}^2)^{1/2} (W_{\text{ly}}^2 + W_{\text{py}}^2)^{1/2} L,$$

where  $h$  is Planck's constant,  $\nu_p$  is the pump laser frequency,  $\sigma_e$  is the stimulated emission cross section,  $\eta_p$  is the pump quantum efficiency (assumed to be unity so that one laser photon is produced for every pump photon), and  $\tau_{\text{fl}}$  is the fluorescence lifetime.  $L$  is the single pass exponential loss in the guide so that the transmission =  $e^{-L}$  and  $W_{\text{l}}$  and  $W_{\text{p}}$  are the average spot sizes for the laser and pump beams, respectively, in the guided ( $x$ ) and unguided ( $y$ ) planes.

From the above equation, we calculate a theoretical threshold value of 9.6 mW, by using an assumed emission cross section of  $1.7 \times 10^{-23} \text{ m}^2$ , which is the figure found by Kaminskii *et al.*,<sup>17</sup> multiplied by 0.58 to account for the fluorescence broadening in the waveguide. This theoretical threshold is significantly lower than our experimental threshold measurement of 91 mW. It is unclear at this stage why there is such a large discrepancy between the theoretical and the experimental threshold power. If there are additional cavity losses produced by butting mirrors onto the guide, this might account for some of this difference.

In summary, we have demonstrated the laser action of a thin-film waveguide grown by PLD. A crystalline Nd:GGG planar waveguide lased at several wavelengths centered around 1.062  $\mu\text{m}$  with an absorbed threshold pump power of 91 mW. The waveguide had a depth of 2.7  $\mu\text{m}$  and a propagation loss of 6 dB/cm. Future experiments involve etching the films to produce channel waveguides which should significantly reduce the pump power threshold.

The authors would like to thank Tom Brown of the Optoelectronics Research Centre for his assistance in the annealing process and Dr. Mark Weller of the Chemistry Department for access to the x-ray diffractometer. D.S.G., A.A.A., and T.J.W. wish to acknowledge the Engineering and Physical Science Research Council for financial support.

<sup>1</sup>J. A. Agostinelli, G. H. Braunstein, and T. N. Blanton, *Appl. Phys. Lett.* **63**, 123 (1993).

<sup>2</sup>D. C. Hanna, J. K. Jones, A. C. Large, D. P. Shepherd, A. C. Tropper, P. J. Chandler, M. J. Rodman, P. D. Townsend, and L. Zhang, *Opt. Commun.* **99**, 211 (1993).

<sup>3</sup>P. J. Chandler, S. J. Field, D. C. Hanna, D. P. Shepherd, P. D. Townsend, A. C. Tropper, and L. Zhang, *Electron. Lett.* **25**, 985 (1989).

<sup>4</sup>S. J. Field, D. C. Hanna, A. C. Large, D. P. Shepherd, A. C. Tropper, P. J. Chandler, P. D. Townsend, and L. Zhang, *Electron. Lett.* **27**, 2375 (1991).

<sup>5</sup>S. J. Field, D. C. Hanna, A. C. Large, D. P. Shepherd, A. C. Tropper, P. J. Chandler, P. D. Townsend, and L. Zhang, *Opt. Commun.* **86**, 161 (1991).

<sup>6</sup>S. J. Field, D. C. Hanna, A. C. Large, D. P. Shepherd, A. C. Tropper, P. J. Chandler, P. D. Townsend, and L. Zhang, *Opt. Lett.* **17**, 52 (1992).

<sup>7</sup>B. Ferrand, D. Pelenc, I. Chartier, and Ch. Wyon, *J. Cryst. Growth* **128**, 966 (1993).

<sup>8</sup>G. R. Bai, H. L. M. Chang, and C. M. Foster, *Appl. Phys. Lett.* **64**, 1777 (1994).

<sup>9</sup>D. S. Gill, R. W. Eason, J. Mendiola, and P. J. Chandler, *Mater. Lett.* **25**, 1 (1995).

<sup>10</sup>M. Ezaki, H. Kumagai, K. Kobayashi, K. Toyoda, and M. Obara, *The Pacific Rim Conference on Lasers and Electro-Optics*, Chiba, Japan, 1995 (unpublished), p. 620.

<sup>11</sup>Inorganic Crystal Structure Database, Daresbury Laboratory, U.K.

<sup>12</sup>D. L. Wood and K. Nassau, *Appl. Opt.* **29**, 3704 (1990).

<sup>13</sup>Powder diffraction file Inorganic, JCPDS 13-493 (1973).

<sup>14</sup>R. C. Weast, *Handbook of Chemistry and Physics*, 70th ed. (CRC, Boca Raton, Fla. 1989), p. F-187.

<sup>15</sup>H. Nishihara, M. Haruna, and T. Suhara, *Optical Integrated Circuits* (McGraw-Hill, New York, 1989), p. 235.

<sup>16</sup>W. A. Clarkson and D. C. Hanna, *J. Mod. Opt.* **36**, 483 (1989).

<sup>17</sup>A. A. Kaminskii, V. V. Osiko, S. E. Sarkisov, M. I. Timoshechkin, E. V. Zharikov, J. Bohm, P. Reiche, and D. Schultze, *Phys. Status Solidi* **49**, 305 (1978).